Available online at www.sciencedirect.com

ScienceDirect

Procedia Earth and Planetary Science 15 (2015) 560 – 565

Procedia
Earth and Planetary Science

World Multidisciplinary Earth Sciences Symposium, WMESS 2015

The Numerical Analysis of the Capping Inversion Effect in a Convective Boundary Layer Flow on the Contaminant Gas Dispersion

Hiromasa Nakayama[a]*, Tetsuya Takemi[b], Haruyasu Nagai[a]

[a]*Japan Atomic Energy Agency, Ibaraki, Japan*
[b]*Disaster Prevention Research Institute, Kyoto University, Kyoto, Japan*

Abstract

Contaminant gas dispersion is of great concern to public health and social security. In the atmosphere, heating and cooling within a boundary layer due to the daily solar cycle result in a temperature differences, which introduces buoyancy forcing. Especially, a convective boundary layer (CBL) capped by a temperature inversion is one of the common cases in the atmospheric boundary layers during daytime conditions. Wind tunnel experimental studies have focused on the characteristics of plume dispersion under a certain thermal condition in a CBL flow. However, CBL flows have shear- and/or buoyancy-driven flows depending on atmospheric stability conditions and the influence of CBLs on plume dispersion behaviours has not been fully discussed. In this study, we performed numerical simulations of CBL flows capped by a temperature inversion with a wide range of atmospheric stability conditions and categorized distribution patterns of plume concentrations. It is found that the critical value of u_*/w_* in which the patterns of plume dispersion are different is around 0.4.

Peer-review under responsibilty of the Organizing Commitee of WMESS 2015.

Keywords: Numerical analysis; large-eddy simulation; contaminant gas dispersion; convective boundary layers; capping inversion effects.

1. Introduction

Contaminant gas dispersion resulting from accidental release from industrial areas or intentional release of CBRN (chemical, biological, radiological, or nuclear) agent is of great concern to public health and social security.

* Corresponding author. Tel.: +41 21 69 30818.
E-mail address: nakayama.hiromasa@jaea.go.jp

Peer-review under responsibilty of the Organizing Commitee of WMESS 2015.
doi:10.1016/j.proeps.2015.08.101

In the atmosphere, heating and cooling within a boundary layer due to the solar cycle during a day results in temperature differences, which introduce buoyancy forcing. Especially a convective boundary layer (CBL) capped by temperature inversion is one of the common cases of atmospheric boundary layers during daytime conditions. For simulating plume dispersion under various thermal conditions, there are typically two approaches: one is a wind tunnel experimental technique, and the other is a numerical simulation based on computational fluid dynamics (CFD). It is well known that wind tunnel experiments are a reliable tool. Recently, wind tunnel experiments have been conducted to investigate the influence of a convective boundary layer capped by a temperature inversion on plume dispersion behaviours of a contaminant gas and relative release height to the capping inversion height on the longitudinal distribution patterns of concentration (Fedorovich and Thater, 2002). However, these studies have focused on the characteristics of plume dispersion under a certain thermal condition. CBL flows have shear- and/or buoyancy-driven flows depending on atmospheric stability conditions. The influence of CBLs on plume dispersion behaviours has not been fully discussed depending on thermal conditions.

On the other hand, with the rapid development of computational technology, the CFD using large-eddy simulation (LES) technique has been evolving as an alternative to wind tunnel experiments. LES models resolve large-scale turbulent motions and model only small-scale motions, which has been recognized as a helpful tool for providing a better understanding of the physical mechanism of airflow motions, heat and mass transfer.

In this study, we perform CFD simulations of various CBL flows capped by a temperature inversion using LES technique and compare the computed results with the experimental wind tunnel data. Then, we categorize distribution patterns of plume concentrations depending on various atmospheric stability conditions.

2. Numerical method

2.1 Dataset of wind tunnel experiments

In this study, we compare four types of CBL flows with a temperature inversion by Ohya and Uchida (2004) with experimental data. The experimental conditions are shown in Table 1. The Reynolds numbers Re defined as $U_\infty Z_i/\nu$ are 28,000, 25,000, 19,400, and 18,400 for cases1, 2, 3, and 4, respectively. Here, U_∞, Z_i, and ν are the free-stream velocity, inversion height and kinematic viscosity coefficient, respectively. The bulk Richardson numbers Ri_b defined as $gZ_i\Delta\Theta/\Theta_0 U_\infty^2$ are –0.23, -0.28, -0.45, and -0.74 for the four cases, respectively. Here, g, Θ_0, and $\Delta\Theta$ are gravitational acceleration, average absolute temperature in the boundary layer and temperature difference between temperature of ambient air Θ_∞ and surface temperature Θ_s.

In their experiments, first, air flow with a temperature profile was imposed at the entrance of the test section. The convective boundary layer was produced by an obstacle and the entire floor was heated. In their study, turbulence characteristics obtained at a downwind distance of 24.1 Z_i from the text section was investigated.

Table 1. Experimental and computational conditions.

Method	Parameter	Case 1	Case 2	Case 3	Case 4
Experiment	Re_{zi}	28,000	25,000	19,400	18,400
	Re_{zi}	-0.23	-0.28	-0.45	-0.74
LES	Re_{zi}	26,000	24,000	19,000	18,000
	Re_{zi}	-0.21	-0.26	-0.42	-0.69

2.2 Numerical model

The model used here is a LOcal-scale High-resolution atmospheric DIspersion Model using LES (LOHDIM-LES) developed by the Japanese Atomic Energy Agency (Nakayama et al., 2014). The basic equations are the filtered continuity and Navier-Stokes equation, the temperature transport equation under the Boussinesq approximation and concentration transport equation. The subgrid scale (SGS) turbulent effect is represented by the standard Smagorinsky model (1963) with a constant value of 0.1.

The SGS scalar flux is also parameterized by an eddy viscosity model and the turbulent Prandtl and Schmidt numbers are both constant values of 0.71.

The coupling algorithm of the velocity and pressure fields is based on the marker-and-cell method with the second-order Adams-Bashforth scheme for time integration. The Poisson equation is solved by the successive over-relaxation method. For the spatial discretization in the basic equations, a second-order accurate central difference scheme is used. However, for the advection term of the concentration transport equation, cubic interpolated of pseudo-particles (Takewaki et al., 1985) is used.

2.3 Computational settings

The approach to generate CBL flows by a temperature inversion is the same as in our previous study (Nakayama et al., 2014). First, a driver region is set to generate a basic turbulent boundary layer flow by a recycling technique of Kataoka and Mizuno (2002) at the upstream part of the model domain. At the inlet boundary, a mean wind velocity profile of the power law 0.14 is imposed. At the recycle station, a nearly target temperature profile is imposed, and CBL flows are spatially developed.

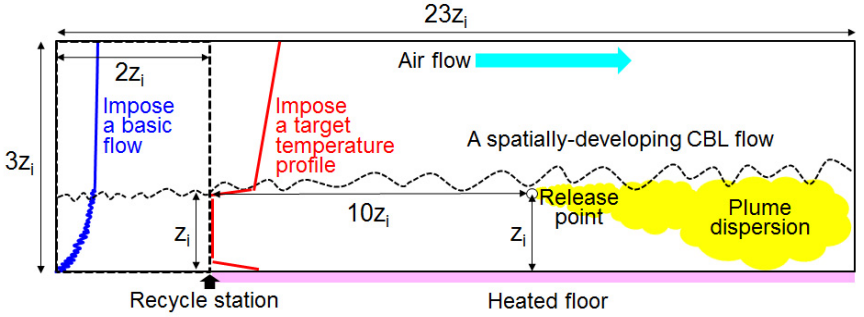

Fig. 1. Numerical model for plume dispersion in thermally stratified boundary layers.

For the velocity field, the Sommerfeld radiation condition is applied at the exit. At the top, a free-slip condition is imposed for streamwise and spanwise velocity components, and the vertical velocity component is set to be zero. At the side, a periodic condition is imposed. At the ground surface, a no-slip condition is imposed for each velocity component. For temperature and concentration fields, a zero-gradient condition is imposed at all boundaries. However, for the temperature field, the surface temperature is set to Θ_∞. The time step interval $\Delta t U_\infty / Z_i$ is about 0.003 (Δt: time step). The length of the simulation run to calculate the time averaged values TU_∞ / Z_i (T: averaging time) is 200. The length of the simulation run before releasing a plume is 300.

The model size and the number of grid points are $23.0\,Z_i \times 5.0\,Z_i \times 3.0\,Z_i$ and 1150×250×114 in the streamwise, spanwise and vertical directions, respectively. The streamwise and spanwise grid spacing is uniform and the vertical grid spacing is stretched from $0.002\,Z_i$ to $0.09\,Z_i$ for each case. Re and Ri_b are set to nearly the same values as those of the experiments shown in Table 1. The release point of a tracer gas is set at a downwind distance of $12.0\,Z_i$ downstream from the inlet boundary and elevated with a height of $z/Z_i = 1.0$ for each case.

3. Results

3.1 Flow field

Figure 2 compares the LES results of turbulence statistics with the experimental data shown by Ohya and Uchida (2004). U_m and Θ_m are mean wind velocity and temperature in the range where those values are constant in the middle part of the CBL. w_* is the convective velocity scale defined as $\left(gQ_s\delta/\Theta_0\right)^{1/3}$. Here, Q_s is the maximum value of vertical heat flux $\overline{w'\theta'}$ near a ground surface. The characteristics such as a nearly constant profile of mean velocity and temperature in the main part of the CBL are in good agreement with the experimental data. The LES

results of Reynolds stress are underestimated especially for cases 3 and 4. However, the tendency to decrease with decrease of Ri_b is the same as the experimental data. The LES results of vertical heat flux increase in the main part of the CBL with decrease of Ri_b. This tendency is also the same as the experimental data. These facts indicate that the LES model provides physically reasonable results depending on atmospheric stability conditions.

In identifying turbulence regime in the CBL flows with shear- and/or buoyancy-driven flows, the ratio of u_* to w_* is usually estimated. Here, u_* is the friction velocity and estimated from the maximum value of the Reynolds stress near the surface. For example, Fedorovich et al. (2001) mentioned that shear-free convective flows become dominant for $u_*/w_* < 0.3$ and longitudinal rolls that are often observed in the shear-driven flows begin to form for $u_*/w_* > 0.35$. Ohya and Uchida (2004) also mentioned that the critical value that can divide CBL flows into two turbulence regimes is around 0.4 from experiments. In our LES, the values of u_*/w_* are 0.51, 0.47, 0.39, and 0.33 for cases 1, 2, 3, and 4, respectively. Therefore, from the critical value shown by Ohya and Uchida (2004) we consider the simulated CBL flows to be weakly unstable where shear-driven flows are dominant for cases 1 and 2, and strongly unstable where buoyancy-driven flows are dominant for cases 3 and 4.

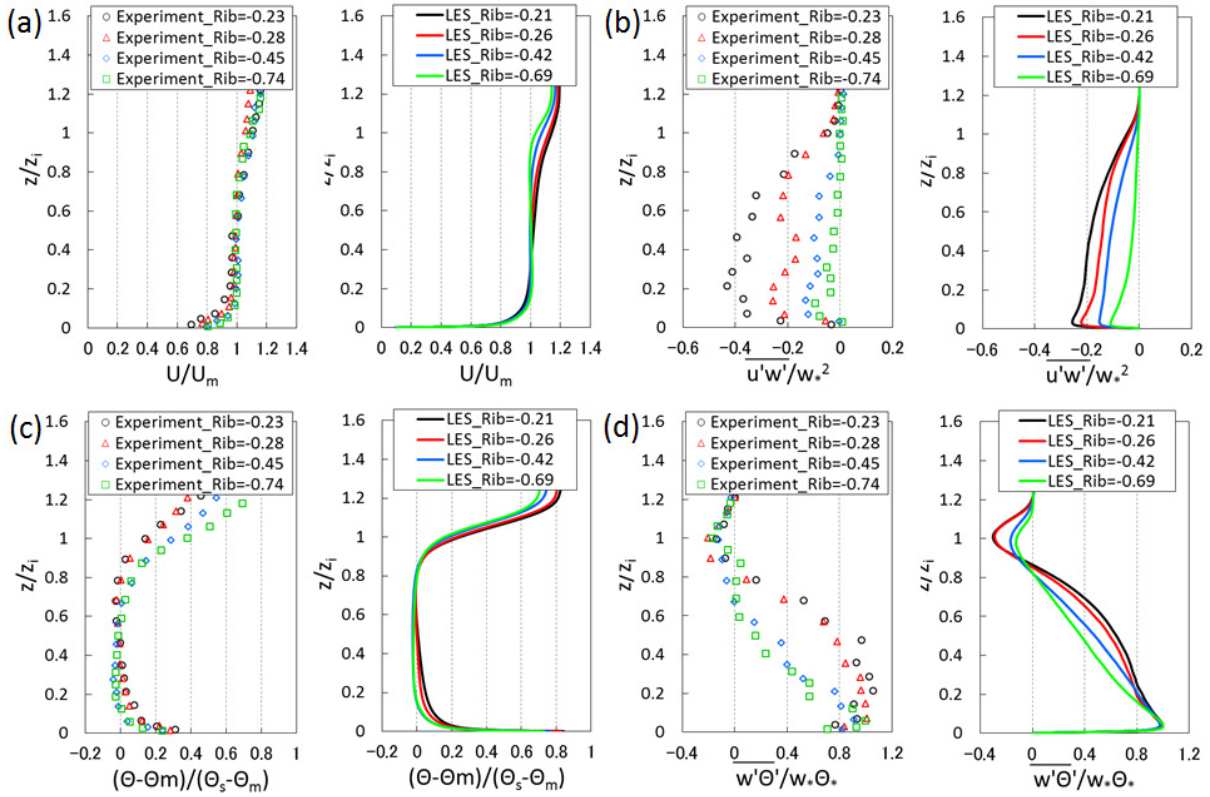

Fig. 2. Vertical profiles of (a) mean velocity, (b) Reynolds stress, (c) mean temperature, and (d) vertical heat flux.

3.2 Dispersion field

Figure 3 shows instantaneous plume dispersion fields for each case. In each case, the upward spreads of the plume are found constrained by blocking effect of the capping inversion. However, the plume is rapidly dispersed downwards for strongly unstable conditions (cases 3 and 4) while the downward spreads are comparatively small for weakly unstable conditions (cases 1 and 2). Figures 4 and 5 show vertical profiles of mean concentrations and

vertical concentration fluxes at each downstream position. For weakly unstable conditions, the downward spreads of the plume gradually become large with downwind distance. The shape of the vertical concentration fluxes is nearly non symmetric and shows sharp peak at the release height at each downstream position. On the other hand, for strongly unstable conditions, the downward plume spreads rapidly become large with downwind distance and the touchdown is observed for $x/z_i \geq 8.0$. The shape of vertical concentration fluxes becomes nearly uniform in the main part of the CBL for $x/z_i \geq 8.0$ due to the active vertical turbulent transport.

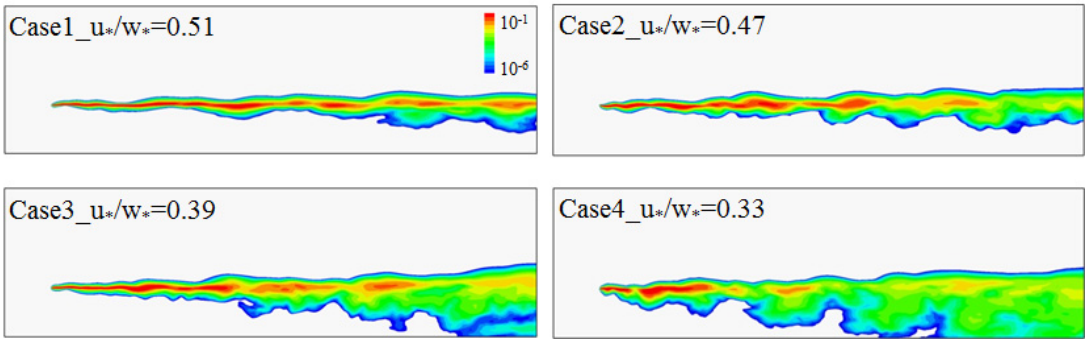

Fig. 3. Instantaneous plume dispersion fields. Colored contours indicate instantaneous concentration values normalized by source concentration.

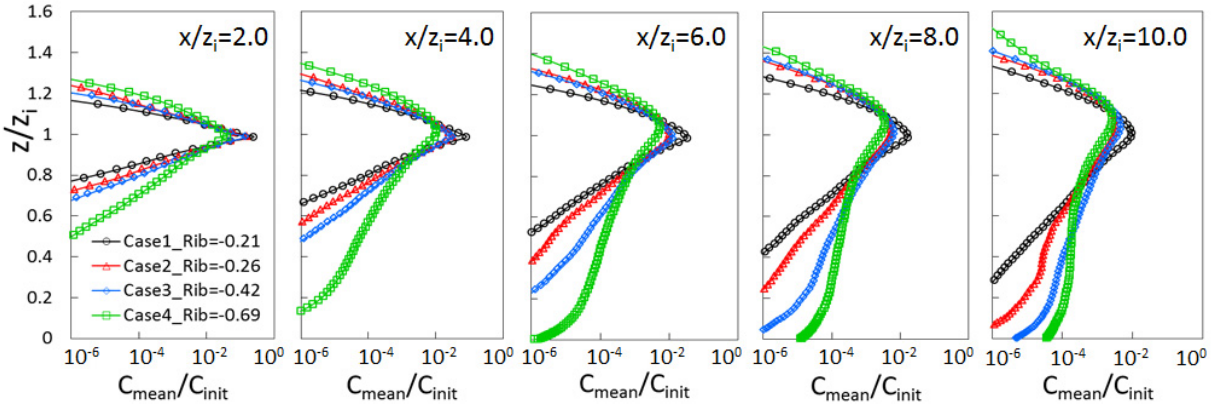

Fig. 4. Vertical profiles of mean concentrations at each downstream position.

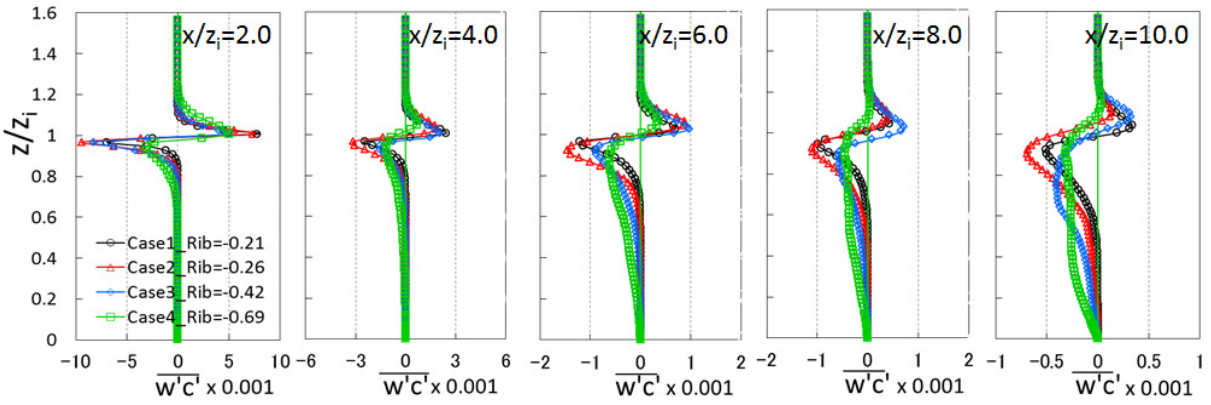

Fig. 5. Vertical profiles of vertical concentration fluxes at each downstream position.

4. Conclusions

We performed LESs of CBL flows capped by a temperature inversion with a wide range of atmospheric stability conditions and compared it with wind tunnel experimental data. Although some of the turbulence characteristics are quantitatively different from the experimental data, the distribution patterns depending on atmospheric stability conditions are generally the same as those of the experiments. Then, we investigated the influence of stability conditions on plume dispersion behaviours. For weakly unstable conditions with $u_*/w_* > 0.4$, the downward spreads of the plume gradually become large with downwind distance. The shape of vertical concentration fluxes is nearly antisymmetric at the release height at each downstream position. On the other hand, for strongly unstable conditions with $u_*/w_* < 0.4$, those rapidly become large with downwind distance. The touchdown of the plume is observed for $x/z_i \geq 8.0$. The vertical concentration flux profiles become nearly uniform in the main portion of the CBL due to the active vertical turbulent transport. It can be concluded from these results that the critical value of u_*/w_* in which the patterns of plume dispersion are different depending on atmospheric stability conditions is around 0.4.

Acknowledgement

The study is partly supported by JSPS KAKENHI Grant 26282107.

References

1. Fedorovich, E., Nieuwstadt, F. T. M., Kaiser, R., 2001. Numerical and Laboratory Study of a Horizontally Evolving Convective Boundary Layer, Part II: Effects of Elevated Wind Shear and Surface Roughness, Journal of Atmospheric Sciences, 58, 546–560.
2. Fedorovich. E., Thater. J., 2002. A wind tunnel study of gaseous tracer dispersion in the convective boundary layer capped by a temperature inversion, Atmospheric Environment, 36, 2245-2255.
3. Kataoka, H., and Mizuno, M.: Numerical flow computation around aeroelastic 3D square cylinder using inflow turbulence, Wind and Structures, 5, 379-392, 2002.
4. Nakayama, H., Takemi, T., and Nagai, H., 2014. Large-eddy simulation of plume dispersion under various thermally stratified boundary layers, Advances in Science and Research, 11, 75-81.
5. Ohya, Y., and Uchida, T.: Laboratory and numerical studies of the convective boundary layer capped by a strong inversion, Boundary-Layer Meteorology, 112, 223-240, 2004.
6. Smagorinsky, J.: General circulation experiments with the primitive equations, Monthly Weather Review, 91, 3, 99–164, 1963.
7. Takewaki, H., Nishiguchi, A., and Yabe, T.: Cubic Interpolated Pseudo-particle method (CIP) for solving hyperbolic-type equations, Journal of Computer Physics, 61, 261-268, 1985.